Thermal convection in tilted porous fractures

2002 J. Phys.: Condens. Matter 14 2467

(http://iopscience.iop.org/0953-8984/14/9/334)

INSTITUTE OF PHYSICS PUBLISHING JOURNAL OF PHYSICS: CONDENSED MATTER

J. Phys.: Condens. Matter **14** (2002) 2467–2474 PII: S0953-8984(02)31182-2

Thermal convection in tilted porous fractures

A Medina[1], **E Luna**[1], **C Pérez-Rosales**[1] **and F J Higuera**[2]

[1] Grupo de Medios Porosos y Granulados, Programa de YNF, IMP, AP 14-805, 07730 Mexico, DF, Mexico
[2] ETS Ingenieros Aeronáuticos, Plaza Cardenal Cisneros 3, 28040 Madrid, Spain

Received 22 November 2001
Published 22 February 2002
Online at stacks.iop.org/JPhysCM/14/2467

Abstract

We study theoretically and experimentally the thermal convection in long tilted fractures filled with a porous material (porous layer) embedded in an impermeable solid and saturated with a fluid. The solid is subjected to a constant, vertical temperature gradient and has thermal conductivity larger than that of the saturated porous layer. We discuss different cases of interest in terms of the fracture aspect ratio and the fracture-to-solid conductivity ratio. Analytical expressions for the temperature and velocity profiles of the flow in the porous layer are worked out for low-Rayleigh-number flows.

1. Introduction

A fundamental problem in the area of complex systems is how a confined fluid is destabilized due to inhomogeneities in the temperature field and consequently how this follows an effective flow. A very interesting geometrical configuration where a complex temperature distribution appears is that of a fluid-saturated porous tilted layer embedded in an impermeable solid which is subjected to a vertical temperature gradient [1, 2]. In this configuration the fluid is driven by the buoyancy forces, induced by the gradients developed around the porous layer, generating a convective motion within the porous material. In nature there are many systems where fluids saturate tilted porous layers. For instance, oil- or water-saturated layers are embedded in impermeable rocks subjected to a geothermal temperature gradient [1]. The permeable layers commonly are sandstones while the impermeable surrounding rock is shale. In this case the saturated sandstone may have a thermal conductivity lower than that of the shale and the flow in the permeable layer is produced by the sloping isotherms. In this work we will analyse theoretically and experimentally cases where two fluid-filled fractures are interconnected and where a fracture is filled with a saturated porous material. The fractures have finite lengths and the temperature distribution in the impervious solid is introduced as a boundary condition in order to find the solution of the governing equations for the fluid. Knowledge of the temperature and the velocity profiles is of interest because important phenomena such as contaminant dispersion and diagenesis in the layer depend on fine details of these quantities [1, 2]. The thermal convections in the cases of an infinite porous layer, a

fluid-filled infinite tilted fracture, and a fluid-filled finite tilted fracture, under conditions of lower thermal conductivity of the fluid with respect to that of the solid, have been already treated following different approximations [2–5].

2. Fractured reservoirs

Consider a fractured reservoir of characteristic depth H, consisting of an impermeable rock criss-crossed by a complex system of fractures of different widths b, lengths L, and orientations. Typically $\epsilon = b/H \ll 1$, while L can be of the order of H for the longest fractures or fracture paths, or small compared with H. In the simplest possible model of an oil or water reservoir, the fractures are filled with a fluid or with a fluid-saturated porous medium, and the effective thermal conductivity of the material in the fractures, k_m, is typically small compared with the thermal conductivity of the rock, k_s; i.e., $\delta = k_m/k_s \ll 1$. The vertical geothermal temperature gradient G leads to a characteristic temperature variation $\Delta T = GH$ across the reservoir. The ratio of the thermal resistance of a fracture of width b to the thermal resistance of the rock matrix is measured by $\Delta T_m/\Delta T$, where ΔT_m is the temperature difference across the fracture that would lead to a conduction heat flux $k_m\,\Delta T_m/b$ equal to the heat flux $k_s\,\Delta T/H$ due to the geothermal gradient in the matrix. Two limiting cases can be considered, depending on the value of the ratio ϵ/δ.

2.1. $\epsilon \ll \delta$

The temperature difference ΔT_m is small in the much studied case of $\epsilon \ll \delta$, in which the presence of the fractures does not affect the uniform vertical temperature gradient in the rock, in a first approximation. The condition of continuity of the heat flux normal to a fracture that runs at a local angle ϕ to the horizontal requires that the temperature difference between opposite points on the two surfaces of the fracture scaled with ΔT should be $(\epsilon/\delta)\cos\phi$. The temperature difference that would exist between these points in the absence of a fracture is $\epsilon\cos\phi$. The difference between the two values, $(\delta^{-1} - 1)\epsilon\cos\phi$, is a temperature mismatch introduced by the fracture, which is zero only if $\delta = 1$ or $\phi = \pi/2$. In any other case, the mismatch leads to a temperature perturbation in the solid order ϵ/δ relative to the geothermal temperature distribution. More importantly, the isotherms in the fracture make an angle

$$\gamma = \arctan\left(\frac{(1-\delta)\sin\phi\cos\phi}{\delta + (1-\delta)\cos^2\phi}\right)$$

to the horizontal, so the fluid cannot be in equilibrium in the fracture and a natural convection flow sets in when $\gamma \neq 0$. This flow and its influence on the temperature distribution in the fracture have been analysed, by Woods and Linz [3], for a straight infinitely long fracture filled with a fluid, and, also by Woods and Linz [2], for the case of a fracture filled with a saturated porous medium, while Shaughnessy and Van Gilder [4] gave numerical solutions for finite fractures. The influence of the flow on the temperature distribution can be neglected when the effective Rayleigh number $(b/L)g\alpha\,\Delta T\,b^3/\kappa_m\nu \ll 1$, where α is the coefficient of thermal expansion of the fluid and ν and κ_m are its viscous and thermal diffusivities. (The factor b^3 would change to bK for a saturated porous medium of permeability K.) Flow patterns in domed sheets, modelled as sinusoidal fractures filled with porous media, have been computed by Davies *et al* [7] under these conditions. Further details of the low-Rayleigh-number flow in the fracture and the temperature perturbation in the solid are given in Luna *et al* [5]. These results will be extended to the case of saturated porous media in section 3 below.

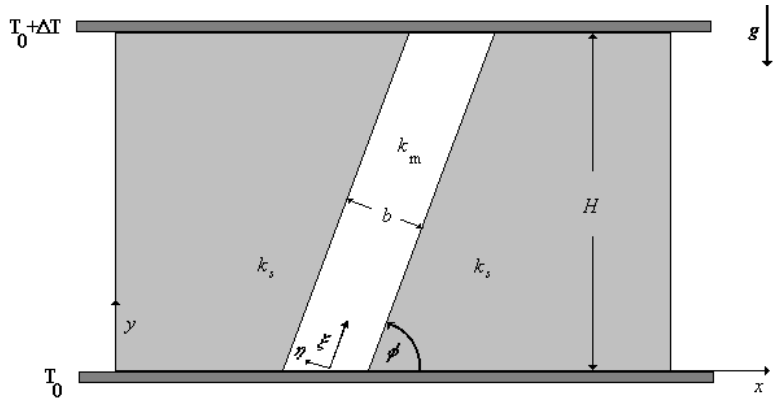

Figure 1. A schematic representation of a tilted fracture embedded in a solid rock of length D, height H, and infinite depth. The angle of tilt of the fracture is ϕ, its width b, and its length is $L = H/\sin\phi$.

2.2. $\delta \ll \epsilon$

In this limiting case, $\Delta T_m \gg \Delta T$, and the available temperature variation across the whole reservoir, $O(\Delta T)$, can only induce a weak heat flux in the fractures. Neglecting this flux, the fractures act as adiabatic barriers for the solid, whose temperature can be computed independently of the flow in the fractures by solving Laplace's equation with adiabatic boundary conditions at the surfaces of the fractures. The temperature distributions on these surfaces, which drive the flow in the fractures, are determined by the solution of the conduction problem. We have investigated this limiting case experimentally and numerically by means of a model reservoir constructed as a horizontal copper slab whose ends are kept at different temperatures by recirculating ethylene glycol from high-thermal-capacity baths. Configurations with a single tilted fracture crossing the slab from end to end (figure 1), as well as systems of fractures like those of figures 2 and 3, have been studied in a copper plate, as the impermeable solid. Glycerine has been used as the working fluid in the fractures. Sample temperature distributions measured with a high-resolution thermal camera are given in figures 4 and 5. In experiments, the typical temperature gradient was $G = 26\ \mathrm{K\ m^{-1}}$. Notice the uniform temperature of the Δ-shaped part of the solid in figure 5, equal to the temperature of the only end of the slab with which it is in contact. Numerical solutions of the conduction problem were computed with a boundary integral-element method. The reduced temperature $\theta = (T - T_0)/\Delta T$, where T_0 and $T_0 + \Delta T$ are the temperatures of the lower and upper ends of the slab, is plotted in figure 6 for a slab with a single fracture at $\phi = 45^\circ$, and in figure 7 for the left-hand side portion of the solid in figure 2. In figure 8 the reduced temperature on the wall of this portion is given. There are also plotted the experimental data obtained from figure 4, which are in a good agreement with the numerical results. On the other hand, the reduced temperatures $\theta_a(\xi)$ and $\theta_b(\xi)$ of the surfaces of the fracture in the first of these configurations are given in figure 9, where the experimental points (symbols) are also plotted. As can be seen, θ_a and θ_b are not linear functions of the distance ξ along the fracture, and their difference depends on ξ. All of this contrasts with the surface temperature distributions for $\epsilon \ll \delta$.

3. Temperature and velocity in a tilted porous fracture

The natural convection flow in tilted fracture filled with a fluid-saturated porous medium is governed by the continuity equation, Darcy's law, and the energy equation. In the Boussinesq

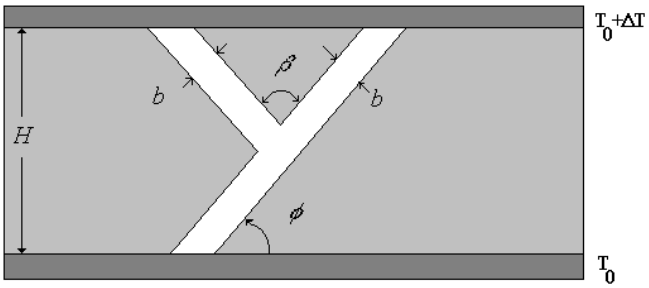

Figure 2. A schematic view of a fracture at an angle ϕ which is intersected perpendicularly by a smaller fracture in the middle part. The widths of both fractures are b.

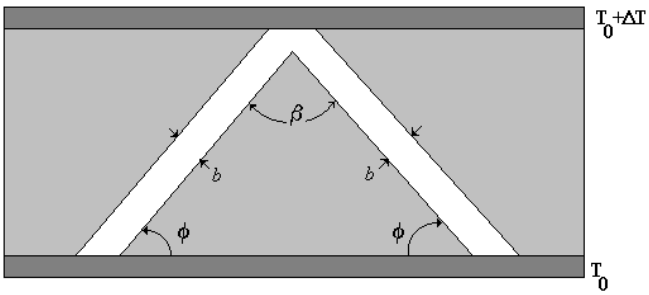

Figure 3. Two interconnected fractures which touch at their upper ends (Δ configuration); the two fractures each make an angle ϕ at their inner end and they made an angle β with each other.

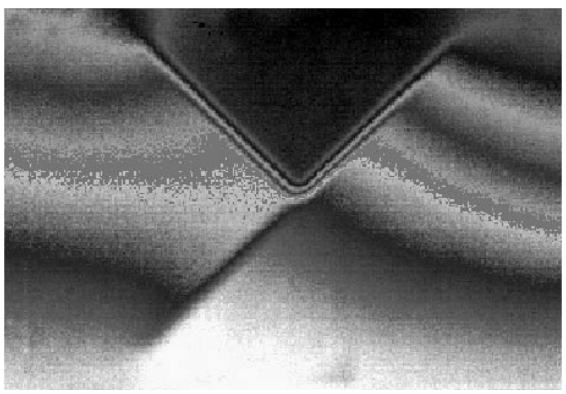

Figure 4. A greyscale thermograph of a copper plate having two fractures like those in figure 2, which have been filled with glycerin.

approximation, these equation can be written in the following non-dimensional form:

$$\boldsymbol{\nabla} \cdot \boldsymbol{v} = 0 \tag{1}$$

$$\boldsymbol{v} = -\boldsymbol{\nabla} P - \boldsymbol{e}_g \theta \tag{2}$$

$$Ra\, \boldsymbol{v} \cdot \boldsymbol{\nabla} \theta = \nabla^2 \theta \tag{3}$$

where $\xi = (\xi, \eta)$ are distances along and normal to the fracture scaled with the width of the fracture b (see figure 1); $\boldsymbol{v} = (u, v)$ are the corresponding components of the velocity scaled with $g\alpha\, \Delta T\, K/\nu$; P is an effective pressure, equal to $p - \rho_0 \boldsymbol{g} \cdot \xi$, scaled with $\rho_0 g \alpha\, \Delta T/b$;

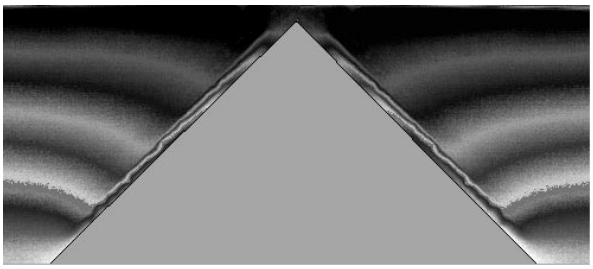

Figure 5. A greyscale thermograph of a copper plate having two interconnected fractures like those in figure 3, which also have been filled with glycerin.

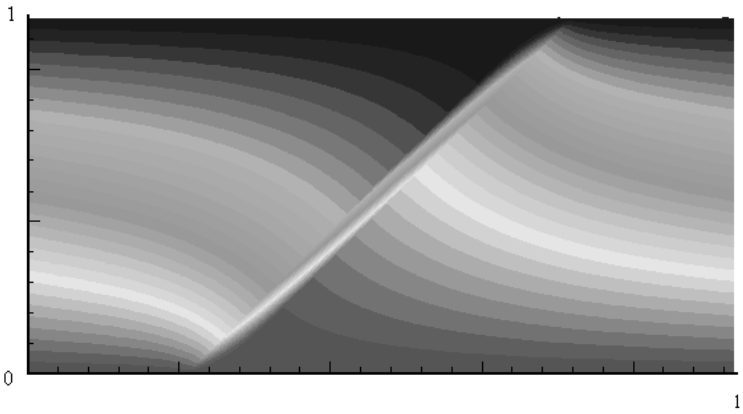

Figure 6. Isotherms in the solid and in the fracture computed numerically for $\delta = 0$ and $\phi = 45^\circ$. In this limit the fracture could be filled with a fluid or with a fluid-saturated porous medium.

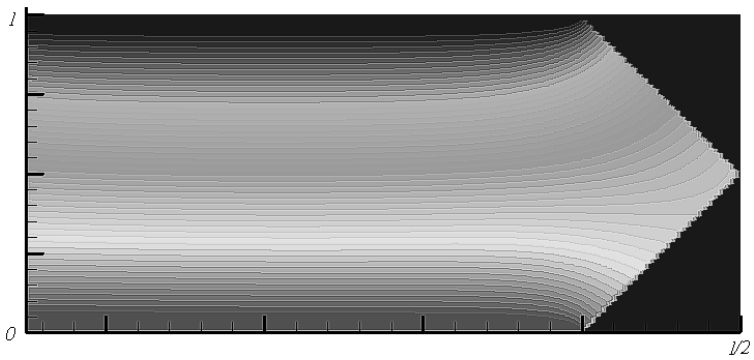

Figure 7. Numerical temperature profiles corresponding to the left-hand side of figure 2. Note the similarity between these profiles and those seen on the left-hand side of the solid in experiments (figure 4).

and θ is the reduced temperature defined above. Here g is the acceleration due to gravity and $\boldsymbol{g} = g\boldsymbol{e}_g$, where $\boldsymbol{e}_g$ is a unit vector pointing downward. The Rayleigh number in (3) is

$$Ra = \frac{g\alpha\,\Delta T\,bK}{\nu\kappa_m}. \tag{4}$$

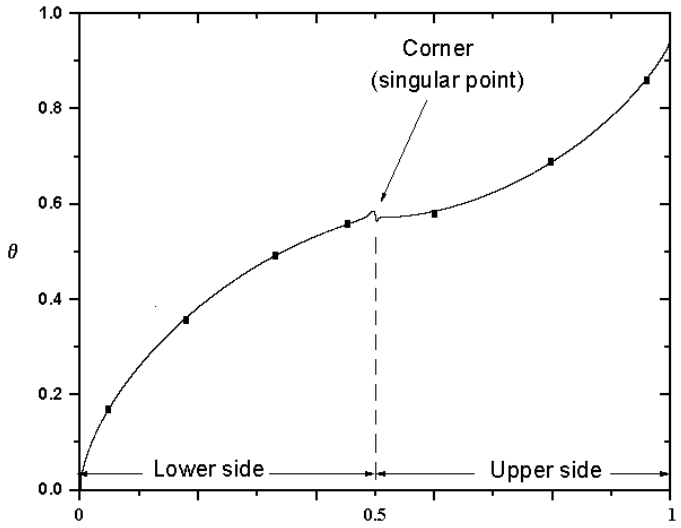

Figure 8. The dimensionless temperature θ along the wall on the left-hand side corresponding to the previous figure. The symbols show the experimental data and the singular point is due to the sudden change (by an angle of 90°) in the slope of this wall.

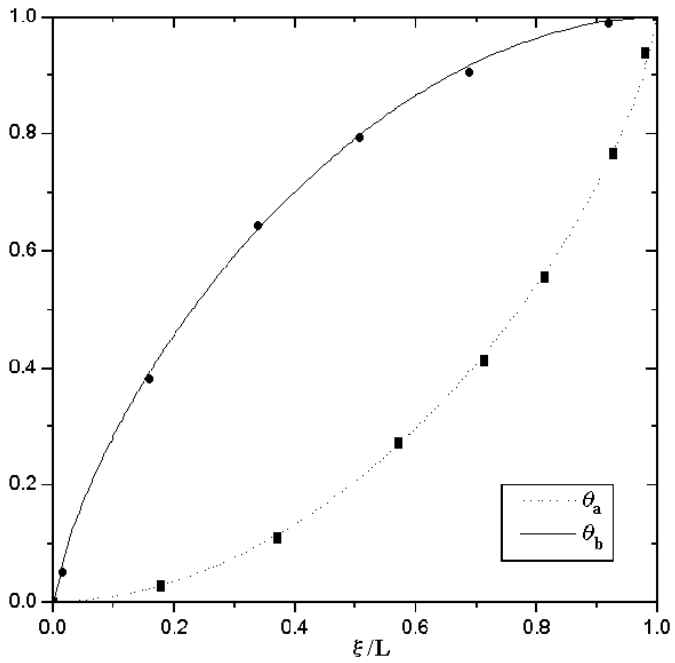

Figure 9. The dimensionless temperature θ along both walls of the fracture as a function of the dimensionless coordinate ξ. The symbols show the experimental data.

These equations are to be solved with the boundary conditions

$$\theta = \theta_a(\xi) \qquad v = 0 \qquad \text{at } \eta = 1/2 \tag{5}$$

$$\theta = \theta_b(\xi) \qquad v = 0 \qquad \text{at } \eta = -1/2 \tag{6}$$

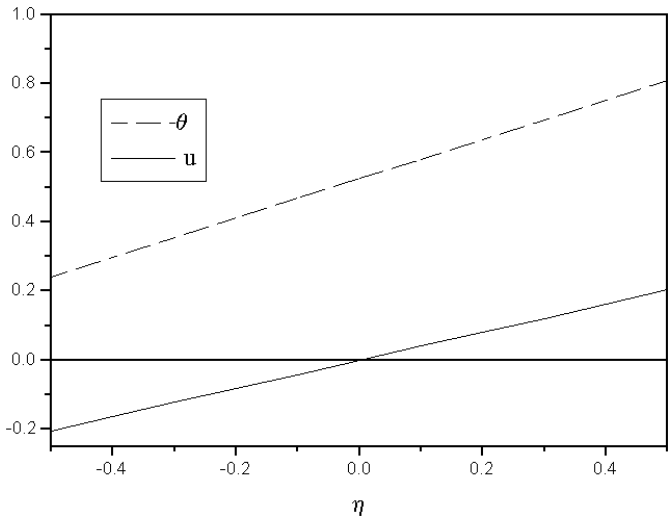

Figure 10. Dimensionless velocity and temperature (u, θ) as functions of η inside the tilted porous layer just at the middle: $\xi/L = 1/2$.

plus appropriate conditions at the upper and lower ends of the fracture, and the condition of zero flow rate

$$\int_{-1/2}^{1/2} u \, \mathrm{d}\eta = 0. \tag{7}$$

We are interested in long fractures, $\Gamma = L/b \gg 1$, with $Ra_{\mathrm{eff}} = Ra/\Gamma \ll 1$. In these conditions, the flow is nearly unidirectional in most of the fracture, $\boldsymbol{v} \approx (u, 0)$, and the energy equation (3) reduces to $\partial^2\theta/\partial\eta^2 = 0$. The solution of this equation with the boundary conditions (5) and (6) is

$$\theta = \tfrac{1}{2}(\theta_a + \theta_b) + (\theta_a - \theta_b)\eta. \tag{8}$$

Carrying this result into (2) and imposing (7), we find

$$u = (\theta_a - \theta_b)\, \eta \sin\phi \tag{9}$$

and

$$\frac{\partial P}{\partial \xi} = (\theta_a + \theta_b) \sin\phi. \tag{10}$$

The solution (8)–(10) is also valid for a curved fracture of local slope $\tan\phi(\xi)$. It is to be contrasted with the hyperbolic profiles for the case of an infinite layer [6]. In figure 10 are plotted the dimensionless velocity (equation (9)) and the temperature (equation (8)), where the values of θ_a and θ_b were obtained from figure 9 just at $\xi/L = 1/2$. These results were proved qualitatively by employing glycerine as the fluid in the porous layer, which was made in a slab filled with glass beads of mean diameter $D = 0.001$ m in a copper plate of 3 cm thickness. The experiments were made at ambient temperature by imposing on the plate a vertical temperature gradient of 4 K in a vertical distance $H = 0.15$ m, so $G = 26\ \mathrm{K\ m^{-1}}$. In the copper plate we have made a slab $b = 0.005$ m wide at $\phi = 45^\circ$. Under these conditions, $K = 700 \times 10^{-6}\ \mathrm{m^2}$ and the glycerine has the thermal expansion coefficient $\alpha = 4.853 \times 10^{-4}\ 1\ \mathrm{K^{-1}}$, viscosity $\nu = 2 \times 10^{-3}\ \mathrm{m^2\ s^{-1}}$, density $\rho = 1260\ \mathrm{kg\ m^{-3}}$, thermal conductivity $k_f = 0.2838\ \mathrm{W\ m^{-1}\ K^{-1}}$ and thermal diffusivity $\kappa_f = 9.346 \times 10^{-8}\ \mathrm{m^2\ s^{-1}}$. The effective thermal diffusivity of the

saturated porous media is $\kappa_m = 5.8 \times 10^{-7}$ m^2 s^{-1}. Therefore, the Rayleigh number has the value $Ra = 57.39$ and the characteristic velocity is $u_c = g\alpha\,\Delta T\,K/\nu = 6.6 \times 10^{-3}$ m s^{-1} which is of the same order of magnitude as that measured in our experiments by following the trace of a fluorescent dye.

4. Conclusions

In this work we analysed the problems of two interconnected fractures embedded in an impermeable solid and of a tilted porous layer. In both cases we have given evidence that the heat-transfer problem in the solid part is very important, and two different limits depending on the value of the ratio ϵ/δ were analysed. Moreover, here we studied the cases of finite fractures when they are touched at the middle and at the upper end. Moreover, the case of a tilted layer saturated with a fluid was also studied in the limit of high thermal conductivity of the solid compared with that of the fluid-saturated porous medium. In this latter case, linear profiles for the velocity and the temperature were obtained, and, because the solutions do not depend on the Rayleigh number, there is always convective motion within the permeable porous layer. Experimental results were found to be in good agreement with the theoretical predictions.

Acknowledgments

This work was supported by the IMP under the projects D.00010 and FIES-98-58-I of the strategic programme *Naturally Fractured Reservoirs*.

References

[1] Phillips O M 1991 *Flow and Reactions in Permeable Rocks* (Cambridge: Cambridge University Press)
[2] Woods A W and Linz S J 1992 *Phys. Rev.* A **46** 4869
[3] Woods A W and Linz S J 1992 *J. Fluid Mech.* **241** 59
[4] Shaughnessy E J and Van Gilder J W 1995 *Numer. Heat Transfer* A **28** 389
[5] Luna E, Córdova J A, Medina A and Higuera F J 2001 *Phys. Lett.* A submitted
[6] Nield D A and Bejan A 1999 *Convection in Porous Media* (New York: Springer)
[7] Davies S H, Rosenblat S, Wood J R and Davies T A 1985 *Am. J. Sci.* **285** 207